J.K.A.U.: Earth Sci., vol. 3, Special Issue: 1st Saudi Symp. on Earth Sci., Jeddah, 1989, pp. 377-387 (1410 A.H. / 1990 A.D.)

Utilization of Remote Sensing Technology in Geological Mapping: A Case Study in Part of 'Asir', Southern Arabian Shield

MOHAMMED YOUSEF H.T. QARI*
Dept. of Geological Sciences, Univ. College, London, Gower St., London, England

ABSTRACT. The Landsat Thematic Mapper (TM) scanner records six bands of reflected visible and infrared spectrum and one thermal infrared band, the data from which are available in photographic and digital form. A study area of 225 km^2 in the southern Arabian Shield, was selected to demonstrate the utility of the Landsat TM sensor digital imagery for lithological mapping and structural analysis. The selected area is complex due to polyphase deformation, which had resulted in interference fold patterns and faulting. The major lithologies are: granites, gneisses, metasediments, metavolcanics, and gabbroic rocks.

Several image processing techniques were applied to the TM data, following which visual interpretations and map constructions were performed employing the resulting images. these processing techniques included: band ratioing, decorrelation stretching, and edge enhancement. The results demonstrate that TM data can be used for lithological mapping and structural analysis in well exposed arid regions, and to generate detailed geological maps over large areas by using quantitative remote sensing methods, where prior knowledge is available for part of the area.

Introduction

Remote sensing means the collection and interpretation of information about an object and/or area from a distance utilizing its spectral reflecting or emitting properties.

The study area (Fig. 1), is a part of Asir province, located to the north of Khamis Mushayt City in the southern Arabian Shield (intersection of lat. 18°25'N and long. 42°40'E), and was selected in order to demonstrate the capabilities of the Landsat Thematic Mapper (TM) sensor digital imagery for geological applications. The selection of this area was based on the excellent exposure of a diverse suite of igneous and metamorphic rocks, and on the availability of detailed geological studies on ground (Amlas 1983, Qari 1985) which provided ground cross-checking, *i.e.* ground truth, during this study.

Geological Setting

The geology of the outcrops exposed in the study area is complex because of the repeated folding and intrusions which have affected the area. The major lithological units are: granites, gneisses, metasediments, amphibolites, and gabbroic rocks.

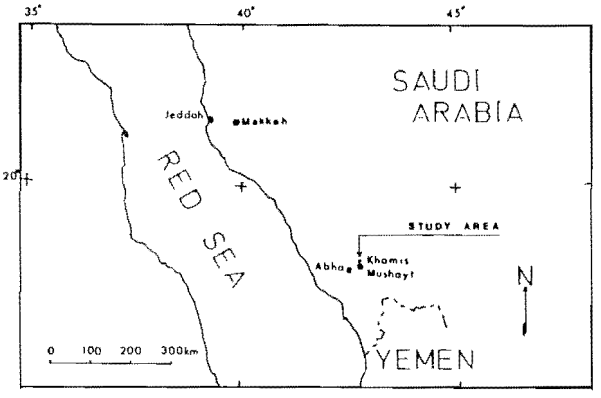

FIG. 1. Location map of the study area.

Granite intrusions are distributed randomly in the

*Permanent Address: Faculty of Earth Sciences, King Abdulaziz University, P.O. Box 1744, Jeddah 21441, Saudi Arabia.

area. Gneisses and layered metamorphic rocks (metasediments and amphibolites) occupy a large portion as well. Gabbro is observed in two places, one is to the southwestern corner and the other filling the synform between the dome and the mushroom structures in the southeastern quarter of the study area (Amlas 1983).

Structurally, the area has been affected by four phases of deformation, D1, D2, D3, and D4. The southeastern quarter of the area is composed of a dome-, synform-, and a mushroom-like structures (Amlas 1983), while in the western half the outcrop pattern is the result of similar interference structures in the polydeformed terrain (Qari 1985, 1989).

Apart from the two detailed studies mentioned above, the only other source of geological information is the 1:100,000 map of Coleman (1973), where broadly defined lithological units were mapped based on aerial photo-interpretation and field checking of some localities (Fig. 2).

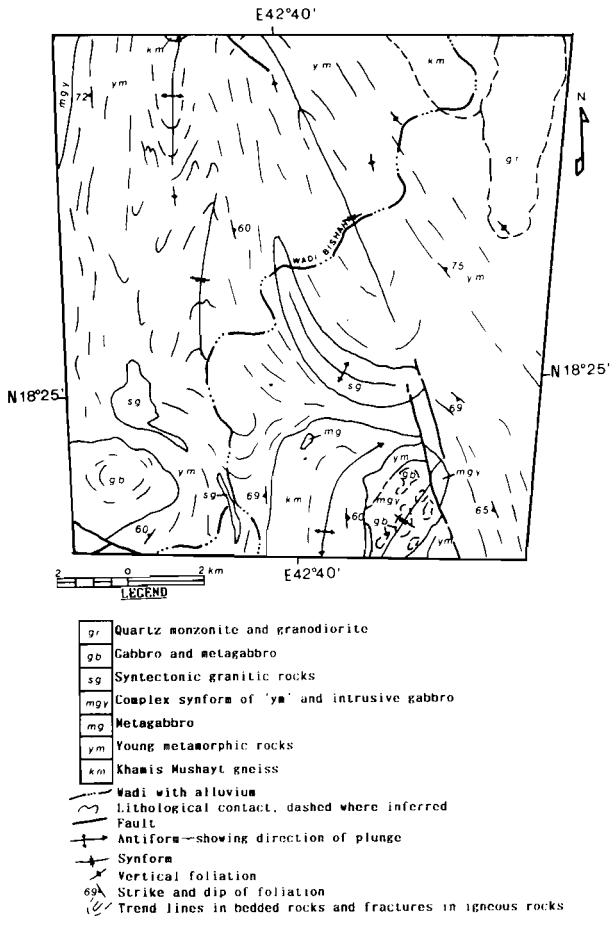

FIG. 2. Published geological map for the study area (after Coleman 1973).

Landsat Digital Data-Analysis and Results

TM Data

A seven band Landsat-4 TM digital image covering 185 by 170 km, acquired on 1 March 1984 (path 167, row 47), was obtained for conducting the quantitative remote sensing studies. The study area sub-scene is 512 × 512 picture-elements (pixels) in size, which is approximately 15 by 15 km, *i.e.* 225 km^2 in area.

The TM scanner records six bands of the reflected visible and infrared spectrum (0.45-2.35 μm) which have image element dimensions of 30 by 30 m on the ground, and one thermal infrared band (10.4-12.5 μm) which has image element dimensions of 120 by 120 m on the ground. Six of the seven bands, 1-5 and 7, are utilized in this study because they are spectrally and spatially significant for geological applications, particularly for lithological mapping and structural analysis (*e.g.* Abrams *et al.* 1985, Rothery 1987, Sultan *et al.* 1987).

Analysis

The spectral reflectance of earth materials is often the most useful criterion for studies in geological remote sensing. Spectral reflectance is a measure, within specific wavelength intervals, of the amount of sunlight reflected by a material, in our case a particular rock-type, and is expressed in images as a photographic tone or colour.

Several techniques for Landsat digital image analysis were applied, which included: band ratioing, decorrelation stretching, and edge enhancement. The prime target was to produce a high quality image hardcopy suitable for geological interpretations, and hence performing map constructions to demonstrate useful applications of TM data for geological studies.

A. Band Ratioing

The rugged nature of the study area and the fluctuation in the topographic relief require an enhancement technique that suppresses these variations. Reflectance ratios have been found to be suitable in this respect (Abrams *et al.* 1977, Blodget and Brown 1982). Therefore, ratioing (dividing) of TM bands was chosen in order to create a Colour Ratio Composite (CRC) image. The technique applied was adopted from Sultan *et al.* (1987).

The TM bands selected are 1,3,4,5, and 7, and the ratio combinations which were applied are: TM band 5/1, TM band 5/7, and TM band (5/4 × 3/4).

The 5/1 band ratio is used to emphasize rocks rich in opaque phases (Hunt *et al.* 1971), the 5/7 band ratio is

used as a measure of the concentration of hydroxyl-bearing minerals, and the (5/4 × 3/4) band combination ratio is used to discriminate regions rich in iron-bearing aluminosilicates (Fig. 3).

(A)

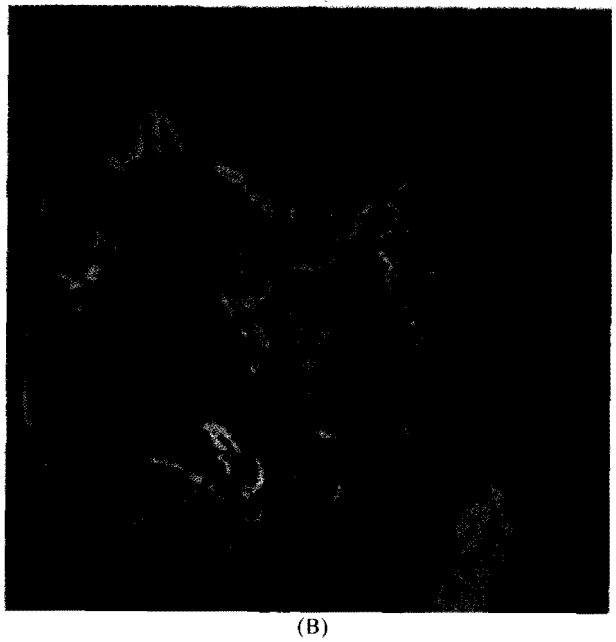

(B)

(C)

FIG. 3. Band ratioing technique used in the study area. A: TM band 5/1, slightly bright areas correspond to regions with high hydroxyl content; B: TM band 5/7, bright areas correspond to regions deficient in opaque phases; C: TM band (5/4 × 3/4), bright areas correspond to regions rich in iron-bearing aluminosilicates.

Gabbroic rock outcrops and amphibole rich metamorphic rocks were identified and discriminated from other rock units observed in the area in the TM band 5/1 and 5/7 ratio images. Amphibolites could be separated effectively from other lithological units in the TM band (5/4 × 3/4) imagery. These distinctions were possible because these rock types have unique brightness patterns on the ratio images and therefore should have unique colours on a CRC image. The granitic and the gneissic rock types have similar brightness on the three ratio images which will result in similar colours on the CRC. The separation between the granitic and the gneissic rock types is difficult, but the field knowledge helped.

The lithological information contained in the three TM band ratio images is integrated into one image. A contrast-stretched CRC is shown in Figure 4. For generating the CRC image, the TM band 5/7 image was assigned to the red component; the TM band 5/1 image to the green component; and the TM band (5/4 × 3/4) image to the blue component. Table 1 indicates the way of expecting the colours on the CRC, based on the mineralogical controls for each of the ratio images discussed previously. For example, the granitic rocks (section F6, Fig. 4), and the gneisses (sections E2, F5, F9, G8, J3, and J5, Fig. 4) are deficient in opaque-, hydroxyl-bearing phases and Fe-bearing aluminosilicates and will result in a green colour in the CRC. Because the gneiss is mixed with other rock types (*e.g.*, amphibolites), these are reflected in the colour of the granitic gneiss on the CRC (blue patches and/or bands of a green colour).

The sediments in the wadis consist primarily of mechanically weathered rock fragments that were transposed from the immediate surroundings. Where the wadi sediments are compositionally similar to the adjacent mountains, the wadis become spectrally indistinguishable on the CRC, such as the case in the small wadis in the granite terrain (section F6, Fig. 4). On the other hand, where the source rock of the sedi-

FIG. 4. A contrast-stretched Colour Ratio Composite (CRC) for the study area. See text for details.

TABLE 1. Explanation of relative colour values in Fig. 4.

Rock type	B 5/7 image bright = red	B 5/1 image bright = green	B 5/4 × 3/4 image bright = blue	Colour in CRC image
Granitic rocks	dark–moderate	bright	dark	Green
Granitic gneiss	dark	bright	dark–moderate	Bluish-green
Amphibolites	moderate–dark	moderate–dark	bright	Bright Reddish-blue
Schistose amphibolites	dark	dark	moderate–dark	Dark Blue
Gabbroic rocks	bright	dark	dark	Red
Intercalated layered metamorphic rocks	moderate–bright	moderate–bright	moderate–bright	Bluish-white

ments in the wadis is compositionally different from the adjacent mountains, the wadis preserve the spectral characteristics of their source rock and are, thus, spectrally distinguishable in the CRC (*e.g.*, Wadi Bishah, sections F4-G2, Fig. 4).

A detailed geological map of the study area was constructed, based on the CRC image (Fig. 5). The field observations were very helpful in making decisions during the construction of the geological map. Comparing the TM-based geological map and the geological information contained in the earlier map by Coleman (1973), it is clear that although there is generally a good agreement between the two maps, there is more detail feature on the TM-based map. For example, the area which is mapped by Coleman as 'young metamorphic rocks' can be resolved into three distinct lithological units on the TM-based map: 1) amphibolites, 2) schistose amphibolites, and 3) intercalated metasediments, amphibolites, and granitic rocks.

Regarding the geological deformations, there were four successive phases which affected the rock types exposed in the study area during Proterozoic time. These four phases produced folds, foliations, and lineations. On the basis of field studies, the four generations were distinguished from each other by their character, orientation, and relationship to one another on various scales (Amlas 1983, Qari 1985).

Because the third phase of deformation was the most dominant, the geological structures resulted are the most prominent and widespread in the study area. Numerous F3 folds were observed, as well as F2 folds throughout the area. The directions of strike of foliations could be delineated on the CRC imagery, particularly in the gneissic and the layered metamorphic lithologies.

Several structures could easily be detected on the CRC imagery. The second-, third-, and fourth-phases of folding (F2, F3, and F4) were clearly detectable in the interference folding patterns visible in the CRC imagery. Several F2 antiformal fold axial traces (Fig. 4, sections D5, D6, and E7), and several F3 antiformal and synformal fold axial traces were extended throughout the area. The F3 traces strike approximately N-S. F4 phase of folding was not easily located although many minor F4 structures were observed (Amlas 1983, Qari 1985). F4 regional doming was predicted when the structural map was constructed (Fig. 6). The F4 axial trace strikes E-W. Micro and meso scale folds were not detectable or extendable on the CRC imagery because their wave lengths are less than the resolution of the imagery. The criterion on which these folds and their axial traces were studied is the changes of the geometry of the banding (foliation planes) of rock units.

Faults were also easily detectable and extendable in the CRC imagery. For example, the gabbroic synformal structure (sections H8 and H9, Fig. 4) has been faulted by a left-lateral strike-slip fault (Fig. 6).

B. Decorrelation Stretching

This technique is based on the statistical analysis of the data (imagery) utilizing Principal Components Analysis (PCA). The PCA (originally known as the Karhunen-Loeve transformation) has been used for many years in various applications, including remote sensing.

Typically, for any pixel in a multispectral original image, the brightness values or Digital Numbers (DNs) are highly correlated from band to band. The

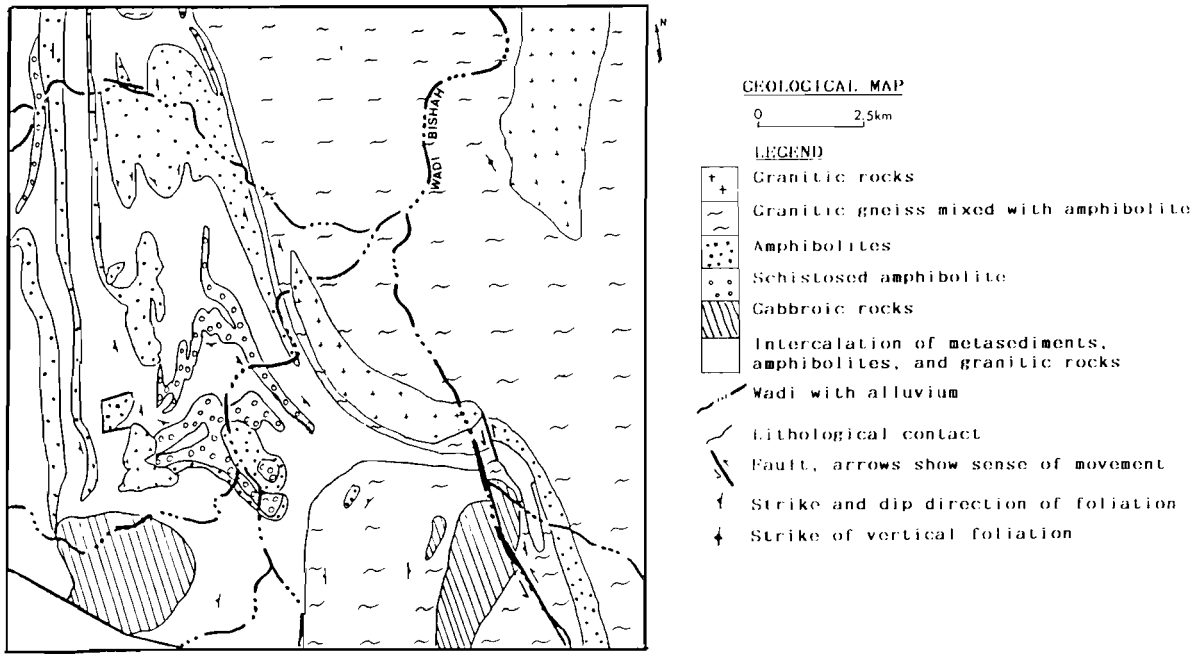

FIG. 5. Geological map constructed from the CRC for the study area.

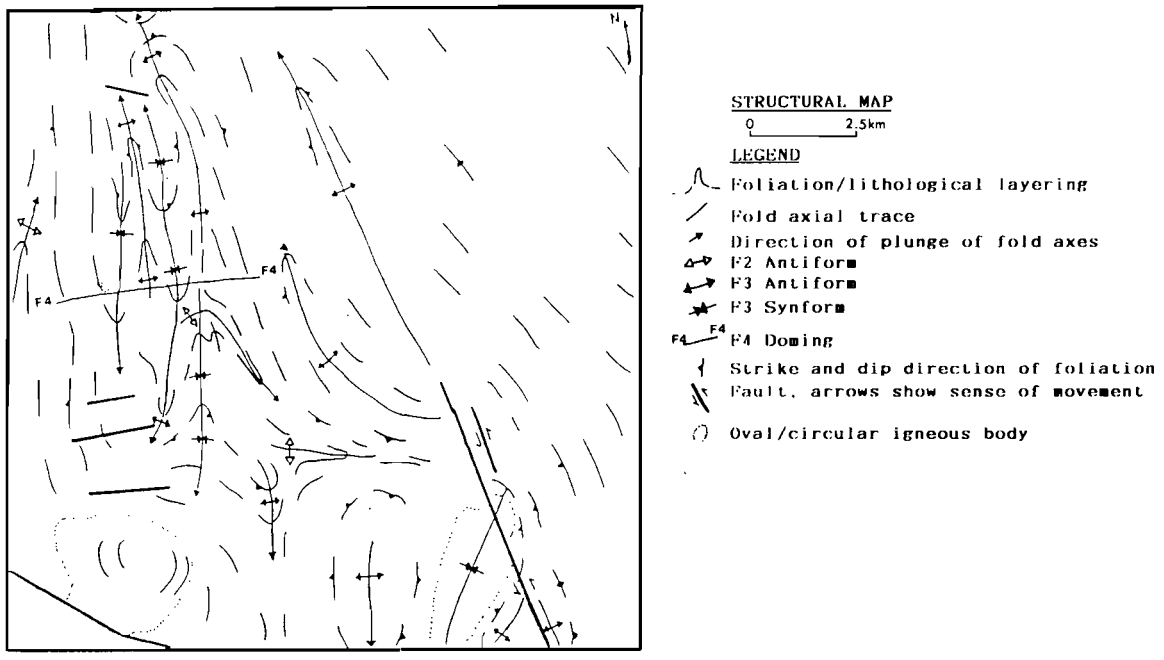

FIG. 6. Structural map constructed from the CRC for the study area.

high correlation implies that there is much redundancy in the data set.

PCA is used to compress multichannel image data by calculating a new coordinate system, *i.e.* by determining a linear transformation that can condense the scene variance in the original data into a new set of variables (axes or principal components). Its aim is to produce decorrelated images and to contain most of

the image information in the first few channels. If we generate a False-Colour Composite (FCC) from any of the three principal components images, by assigning each image to red, green, and blue, respectively, we can not make a full use of colour space. We can achieve this by producing a decorrelation stretched image (Soha and Schwartz 1978). Decorrelation stretching is becoming widely used in geological remote sensing and yielding good results (Abrams *et al.* 1985, Gillespie *et al.* 1986 and Rothery 1987 and 1988). The technique applied in the present study follows the procedure of Rothery (1988), using TM bands 7, 5, and 4.

The TM band 7,5,4-red, green, blue decorrelation stretched FCC image of the study area is shown in Fig. 7. The gabbroic rocks are shown in blue hues (sections B9, B10, C9, and C10), which must not be confused with the blue patches along wadis which are vegetation areas. Granite is the best discriminated lithological unit. The granitic outcrops are shown in bright white hues (*e.g.* sections E5, F7, and I2), while the amphibolitic rocks display a mixture of colours (greenish, brownish, and reddish brown). The schistose amphibolite differs from the amphibolitic unit in that the colour is mostly reddish brown (section D5). The granitic gneiss tends to be white, but because it is mixed with amphibolites, the colour shows brownish red hues on a white background (*e.g.* sections E1, E3, F8, and I8). It takes on a yellow hue where it is rich in metasediments in the intercalated unit (*e.g.* sections A10, B1, and C5).

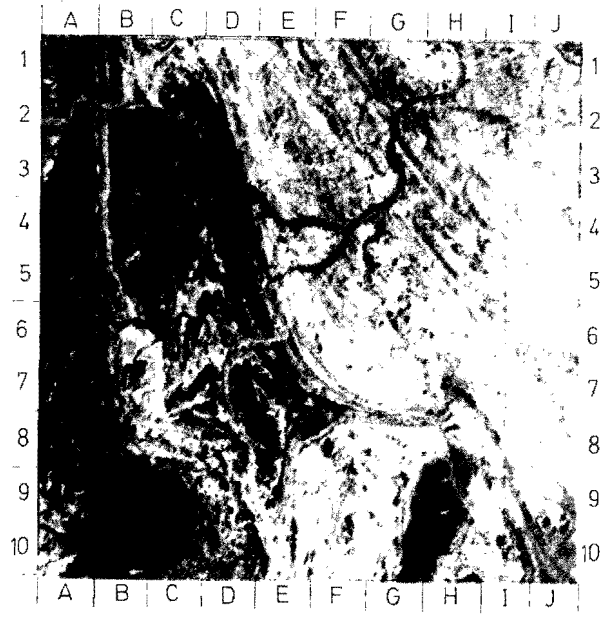

FIG. 7. Decorrelation stretched False Colour Composite (FCC) for the study area. See text for details.

The main wadis are well distinguished in the FCC, because they are different in composition from the surroundings and, hence, differ in spectral characteristics (*e.g.* Wadi Bishah, sections F4 and G2, Fig. 7).

The FCC image produced by this technique permits a geological map similar to Fig. 5, and also a pattern of structures similar to that from the band ratioing technique.

C. Edge Enhancement

Landsat images are especially suited for lineament analysis in relatively high relief areas, where fractures are highlighted by shadowing and appear on the images as linear boundaries. The boundaries mark changes from one range of DN to another, and this is represented by a steep or even vertical gradient, giving rise to edges. These may be shadow effects giving information on topographic features, or may be tectonic features, such as faults or joints. Some edges are boundaries between rocks with different properties, but they have been explicitly excluded from this analysis. Lineaments can be defined as "mappable, simple or composite linear features of a surface, whose parts are aligned in a rectilinear or slightly curvilinear relationship and which differ distinctly from the patterns of adjacent features and presumably reflect a subsurface phenomenon" (O'Leary *et al.* 1976).

A certain amount of subjectivity is inevitable in defining and drawing the lineaments. When applying this technique to bring out geological structure, especially lineaments or fractures, other linear features may appear on the imagery, such as foliations, bedding planes, and compositional layering which may also benefit from this enhancement.

In the present study, edge enhancement was achieved by high-pass filtering in order to emphasize higher spatial frequencies. This was done using a convolution operation which is useful in increasing contrast differences for the enhancement of lineaments. Contrast stretching (scaling) is very important after each convolution to render it displayable. TM band 5 (1.55-1.75 μm) was selected for this enhancement, because bare rock exposures have a relatively uniform grey tone on band 5 images and because atmospheric haze penetration is better in this part of the electromagnetic spectrum.

The method used here has been developed from the techniques by Moore and Waltz (1983) and Masuoka *et al.* (1988). The Landsat TM digital image of the study area has been processed using three high-pass directional digital filters to enhance linear features

oriented along the north, northeast, and northwest directions only. These directions are found to be the most informative in this part of the Arabian Shield, where most outcrops are well exposed and there are no human alterations over most of the ground.

A three-step procedure was performed for lineament enhancement. The first step was to increase the contrast of edges that have trends in approximately the desired directions, *i.e.* northwest, north, and northeast, by making the dark side of an edge segment darker and the light side lighter relative to the background. The resulting filtered images are shown in Figure 8A, B, and C.

(A)

(B)

In the second step, all three filtered images were added together and one more scaling was applied (Fig. 8D). The product of this step was regarded as appropriate for visual drawing of the lineaments or fractures. However, a better image was obtained by adding this scaled and filtered image to the original image, and this was the last step of the procedure. The product is shown in Figure 9, which was used for the identification and tracing of lineaments. The steps followed are summarized in Table 2.

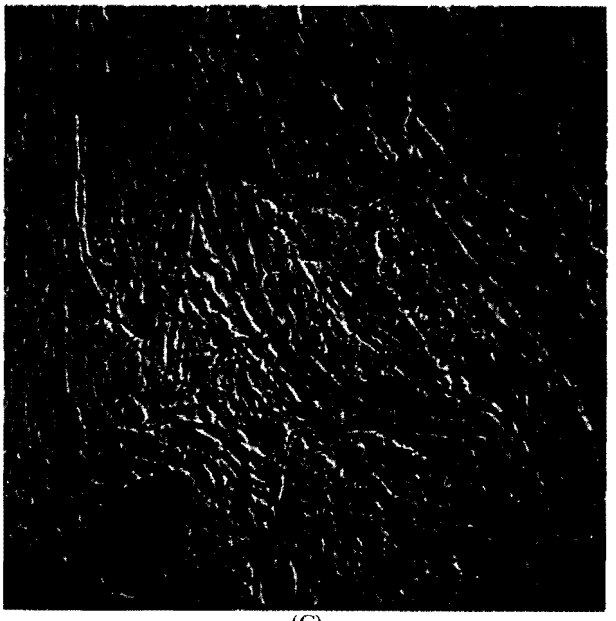

(C)

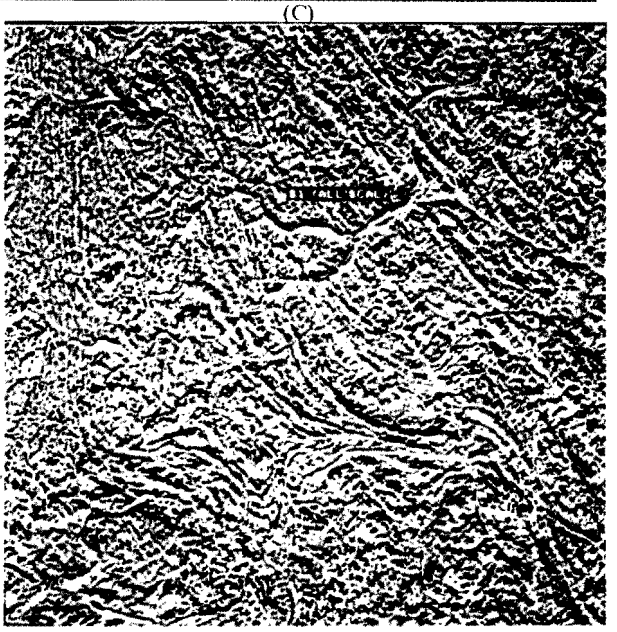

(D)

FIG. 8. Edge enhancement techniques used in the study area. See text for details

The lineaments were identified by visual inspection, and recorded on transparent overlay as ruled straight lines. A remotely sensed geological fracture map was constructed (Fig. 10) based on the knowledge from the field studies, edge enhancement technique image, band ratioing technique image, and decorrelation stretching technique image. When identifying lineaments, what remains relatively constant and reproduc-

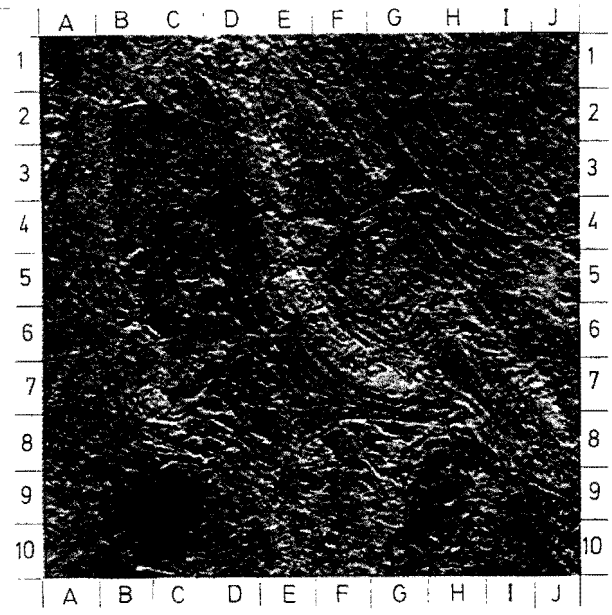

FIG. 9. Directionally enhanced image superimposing TM band 5 for the study area.

TABLE 2. A three-step procedure for producing directionally enhanced images.

Step 1. Derive directional components from original TM band 5. Each pixel in the window is multiplied by the digital value, the final value for the central pixel being the sum of these products. Apply linear stretching (scaling) to each individually.

North-West			North			North-East		
1	1	1	1	1	1	1	1	1
1	-2	-1	1	-2	1	-1	-2	1
1	-1	-1	-1	-1	-1	-1	-1	1

Step 2. Add the previous directionally derived components (filtered images) and apply scaling.
Scaling is a procedure where the lowest digital value is set at 0, and the highest at 255, all intermediate values being distributed through this range.

Step 3. Superimpose (add) directional components of Step 2 to the original TM band 5 image for display and interpretation.

ible is the azimuth of the line drawn rather than its precise location. Thus, the present analysis emphasizes lineament trends rather than the absolute locations of lineaments. Computer processing of lineament data provides an objective method of interpretation. The significance of the lineaments interpreted from images was analyzed by using directional frequency rose diagram. A 10 degree azimuth class interval was used (Fig. 11).

Study of the fracture map (Fig. 10) shows that the lineament frequency is greater in the areas of granitic gneisses and granites (called "granitoid rocks"). The conclusions to be drawn from this diagram are :

- there are many preferred directions for fractures that appear in the study area,
- strong dominance of lineaments in the E-W and N25°W-S25°E directions.
- a general prevailing direction over a wide azimuthal range between N45°-65°E and N55°-65°W.

The lineaments shown on Fig. 10 were counted on a 2.5-km by 2.5-km grid, and the total density was contoured (Fig. 12) to examine the pattern of concentration. Several locations of high concentrations of lineament density are quite apparent. This brings out the high lineament frequency in the area of granitoid rocks where they show as concentrations, particular as two concentrations (>15 and >18) to the upper right of the map (Fig. 12).

An attempt was also made to correlate the observed lineaments (Fig. 10) and mapped faults, using the available detailed geological maps of Amlas (1983) and Qari (1985). Many lineaments were found to accord with faults, while most of the joints were not mapped in the ground surveys. Lineaments or fracture detection, and their subsequence interpretation should not be based on ground studies only. Ground studies can complement spaceborne imagery in order to obtain fruitful results.

Conclusion

Landsat digital TM data covering the visible and reflected infrared spectrum were used to demonstrate the capabilities for geological applications in a well exposed arid region, of the Precambrian southern Arabian Shield. Detailed geological maps were prepared during this study.

Band ratioing and decorrelation stretching techniques were used to demonstrate that TM data can be used for lithological discrimination or mapping and for structural analysis of the poly-phase deformed terrain.

Edge enhancement techniques were used to demonstrate that TM data is useful for revealing lineaments which can be correlated with fractures within the study area. Some of these fractures were known or suspected from ground studies, but the majority were revealed for the first time. Quantitative examinations of the lineaments showed that the study area has several preferential directions; these are E-W, ENE-WSW, WNW-ESE, and N25°W-S25°E.

The results of this study demonstrate that TM data is highly appropriate for geological applications in well-exposed arid regions, and for generating detailed

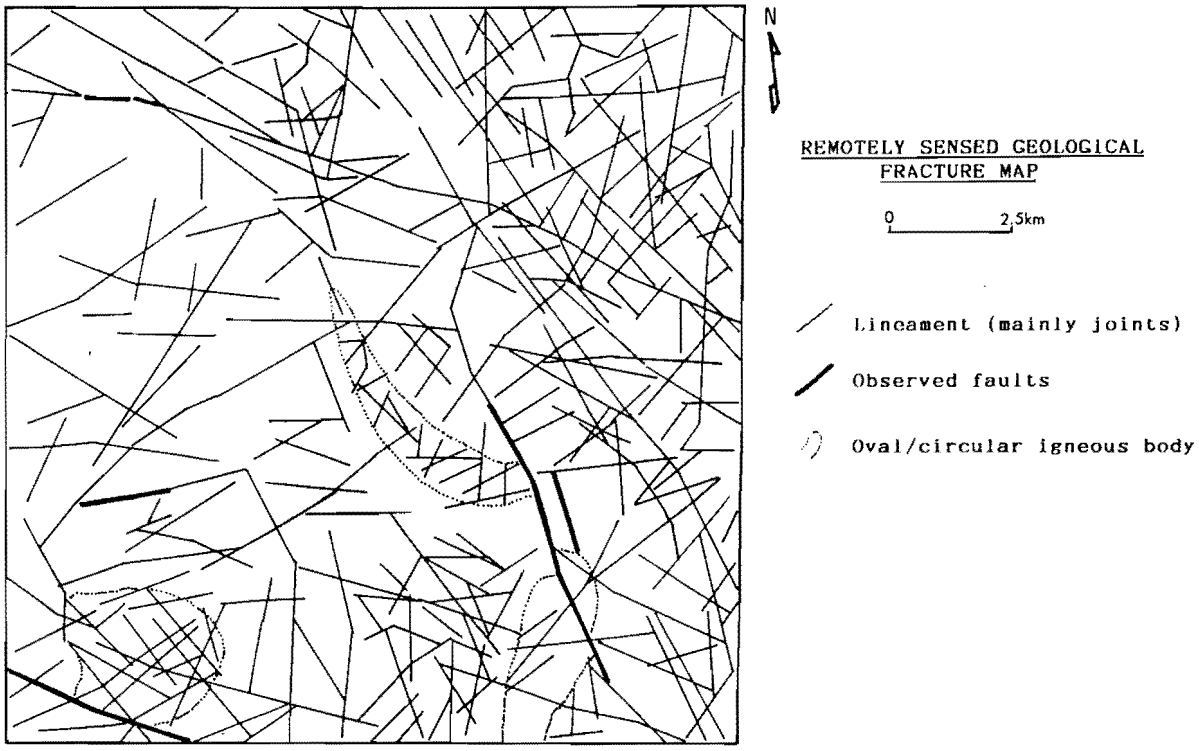

FIG. 10. Remotely sensed geological fracture map for the study area.

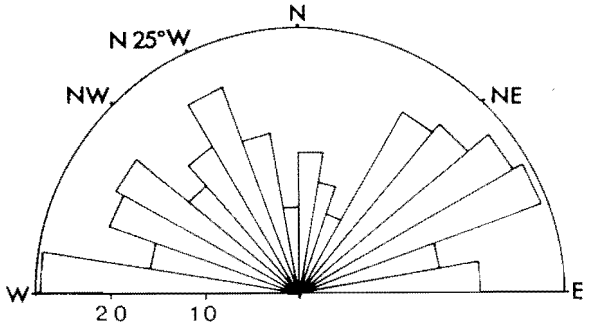

FIG. 11. Rose diagram summarizing strike-frequency distribution of 336 lineaments in Fig. 10.

geological maps over large areas by using quantitative remote sensing methods, where prior knowledge is available for part of the area.

Acknowledgement

This study was carried out at University College London (UCL) as part of a Ph.D. research project, which is sponsored by the King Abdulaziz University, Jeddah, Saudi Arabia. I am very grateful to Dr. Roger Mason, UCL, for his helpful comments, reading the manuscript, and helping in the preparation of this paper. Thanks also due to Dr. M. Tawfiq, Saudi Arabian Directorate General of Mineral Resources (DGMR), Jeddah, for providing the digital imagery and permission for using the DGMR facilities. The imagery was enhanced using the IIS interactive image processing system in the Department of Geography,

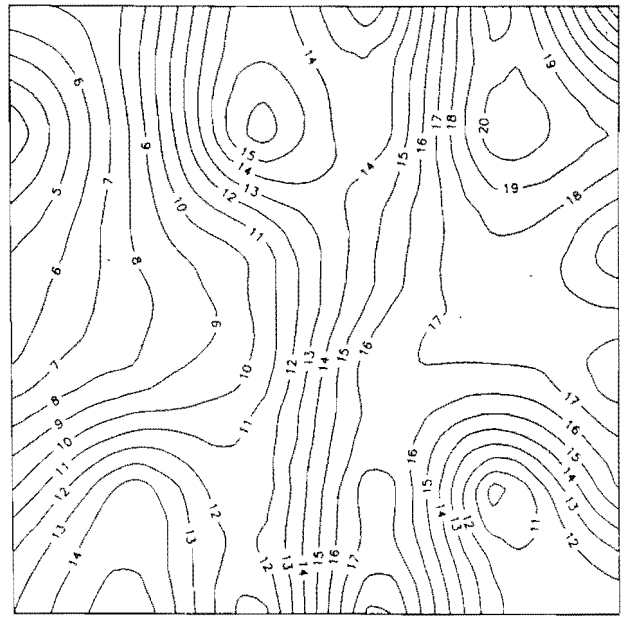

FIG. 12. Fracture density isopleth map. Fracture density is expressed in number of fractures/6.25 km^2.

UCL. Technical support by H. Sheheween and K. Saib, Image Processing Facility, U.S.G.S., Jeddah, is appreciated.

References

Abrams, M.J., Ashley, R.P., Rowan, L.C., Goetz, A.H.F. and **Kahle, A.B.** (1977) Mapping of hydrothermal alteration in the cupprite mining district, Nevada, using aircraft scanner images for the spectral region 0.46 to 2.36 μm, *Geology* **5:** 713-718.

Abrams, M.J., Conel, J.E. and **Lang, H.R.** (1985) *The joint NASA/ Geosat test case project*, Final report. Am. Assoc. Petrol. Geologists.

Amlas, M.M.A. (1983) *Geology and Structures of the Precambrian Rocks North of Khamis Mushayt, Southern Arabian Shield,* M.Sc. thesis, Faculty of Earth Sciences, King Abdulaziz Univ., Jeddah, Saudi Arabia.

Blodget, H.W. and **Brown, G.F.** (1982) Geological mapping by use of computer enhanced imagery in western Saudi Arabia, *United States Geol. Survey Prof. Paper No.* **1153,** U.S.G.S.

Coleman, R.G. (1973) *Reconnaissance Geology of the Khamis Mushayt Quadrangle, Kingdom of Saudi Arabia;* Saudi Arabian Directorate General of Mineral Resources Geologic Map GM-5.

Gillespie, A.R., Kahle, A.B. and **Walker, R.E.** (1986) Color enhancement of highly correlated images. I. Decorrelation and HSI contrast stretches, *Rem. Sens. Environ.* **20:** 209-235.

Hunt, G.R., Salisbury, J.W. and **Lenhoff, C.J.** (1971) Visible and near-infrared spectra of minerals and rocks: III. Oxides and Hydroxides, *Modern Geol.* **2:** 195-205.

Masuoka, P.M., Harris, J., Lowman, P.D. and **Blodget, H.W.** (1988) Digital processing of orbital radar data to enhance geologic structure: examples from the Canadian Shield, *Photogrammetric Engng. Rem. Sen.* **54:** 621-632.

Moore, G.K. and **Waltz, F.A.** (1983) Objective procedures of lineament enhancement and extraction, *Photogrammetric Engng. Rem. Sens.* **49:** 641-647.

O'Leary, D.W., Friedman, J.D. and **Pohn, H.A.** (1976) Lineament, linear, lineation: Some proposed new standards for old terms, *Geol. Soc. Am. Bull.* **87:** 1463-1469.

Qari, M.Y.H.T. (1985) *Structural Analysis of the Proterozoic Rocks Near Janfoor Village (Northwest of Khamis Mushayt), Southern Arabian Shield,* M.Sc. thesis, Faculty of Earth Sciences, King Abdulaziz Univ., Jeddah, Saudi Arabia.

Qari, M.Y.H.T. (1989) Lithological mapping and structural analysis of Proterozoic rocks in part of the southern Arabian Shield using Landsat images, *Int. J. Rem. Sens.* **10:** 499-503.

Rothery, D.A. (1987) Improved discrimination of rock units using Landsat Thematic Mapper imagery of the Oman ophiolite, *J. Geol. Soc. Lond.* **144:** 587-597.

Rothery, D.A. (1988) MOMS-01 used synergistically with Landsat TM, *4th Int. Symp. on Spectral Signatures of Objects in Remote Sensing, Aussois, France.*

Soha, J.M. and **Schwartz, A.A.** (1978) Multispectral histogram normalization and contrast enhancement, *Proc. 5th Canadian Symp. on Remote Sensing, Victoria, B.C.*, 86-93.

Sultan, M., Arvidson, R.E., Sturchio, N.C. and **Guinness, E.A.** (1987) Lithologic mapping in arid regions with Landsat thematic mapper data: Meatiq dome, Egypt, *Geol. Soc. Am. Bull.* **99:** 748-762.

استخدام تقنية الاستشعار عن بعد في إعداد الخرائط الجيولوجية . دراسة حالة في جزء من عسير ، جنوبي الدرع العربي

محمد يوسف هداية الله قاري*

قسم العلوم الجيولوجية ، كلية لندن الجامعية ، لندن ، إنجلترا

المستخلص . يسجل « الراسم الثيماتي » على متن « لاندسات » ستة نطاقات طيفية مرئية منعكسة ودون الحمراء ونطاقًا واحدًا حراريًا دون الحمراء . ويمكن الحصول على تلك البيانات على هيئة صور فوتوغرافية أو أشرطة رقمية للعمل في الحاسب الخاص بمعالجة الصور الفضائية .

مساحة منطقة الدراسة ٢٢٥ كم^2 في الجزء الجنوبي من الدرع العربي . اختيرت تلك المنطقة لإظهار فائدة الصور الرقمية للراسم الثيماتي في إعداد الخرائط الجيولوجية والتفسيرات البنائية (التركيبية) .

المنطقة المختارة للدراسة معقدة من الناحية الجيولوجية ، إذ تعرضت لعدة أطوار من التشوهات نتج عنها أنماط متداخلة من الطيَّات والفوالق . أهم الصخور المكونة للمنطقة : الجرانيت ، النَّيس ، الصخور الرسوبية والبركانية المتحولة ، والجابرو .

تم تطبيق عدة طرق رقمية لمعالجة صور بيانات الراسم الثيماتي ، وتبع ذلك تفسيرات وعمل خرائط باستخدام تلك الصور الناتجة من تطبيق تلك الطرق المختلفة والتي تضمنت :

- تقسيم النطاقات الطيفية Band Ratioing .
- التمديد غير المترابط Decorrelation Stretching .
- تحسين الحدود (الحرف) Edge Enhancement .

أظهرت النتائج أن بيانات الراسم الثيماتي يمكن استخدامها في إعداد الخرائط الجيولوجية والتفسيرات البنائية في المناطق الجافة ذات المكاشف الجيدة ، وكذلك في إعداد خرائط جيولوجية تفصيلية لمناطق شاسعة باستخدام طُرق الاستشعار عن بُعد بشرط توافر معلومات لأجزاء صغيرة من تلك المناطق .

* العنوان الدائم : كلية علوم الأرض ، جامعة الملك عبد العزيز ، جدة ، المملكة العربية السعودية .